JOURNAL OF GUIDANCE, CONTROL, AND DYNAMICS
Vol. 28, No. 3, May–June 2005

Attitude and Orbit Control of a Very Large Geostationary Solar Power Satellite

Bong Wie*
Arizona State University, Tempe, Arizona 85287-6106
and
Carlos M. Roithmayr†
NASA Langley Research Center, Hampton, Virginia 23681-2199

Design of an attitude- and orbit-control system is presented for a 3.2 × 3.2 km geostationary solar-array platform with an area-to-mass ratio of 0.4 m^2/kg. The proposed control-system architecture utilizes electric thrusters for integrated attitude and orbit eccentricity control by counteracting, simultaneously, attitude-disturbance torques and a large orbital perturbing force. Significant control–structure interaction, possible for such a very large flexible structure, is avoided by employing a low-bandwidth attitude-control system. However, a concept of persistent-disturbance accommodating control is utilized to provide precision attitude control in the presence of dynamic modeling uncertainties and persistent external disturbances.

I. Introduction

RENEWED interest in space solar power is spurring reexamination of the prospects for generating large amounts of electricity from large-scale space-based solar power systems. In Refs. 1 and 2, Peter Glaser first proposed the satellite solar power station (SSPS) concept in 1968, and he received a U.S. patent on a conceptual design for such a satellite in 1973. As a result of a series of technical and economic feasibility studies by NASA and the Department of Energy in the 1970s, an SSPS reference system was developed in the late 1970s. The 1979 SSPS reference system, as it is called, featured a very large solar-array platform (5.3 × 10.7 km) and a double-gimbaled microwave-beam-transmitting antenna (diameter 1 km). The total mass was estimated to be 50×10^6 kg. A ground- or ocean-based rectenna (rectifying antenna) measuring 10 × 13 km would receive the microwave beam on the Earth and deliver up to 5 GW of electricity.

In 1995, NASA revisited the space solar power (SSP) concept to assess whether SSP-related technologies had advanced enough to alter the outlook significantly on the economic and technical feasibility of space solar power. The "Fresh Look" study, conducted by NASA during 1995–1997 and reported in Ref. 3, found that in fact a great deal had changed and that multimegawatt SSP satellites appear viable, with important spacecraft-to-spacecraft applications. The study also found that ambitious research, technology development, and validation over a period of perhaps 15–20 years are required to enable SSP concepts to be considered "ready" for commercial development.

Recent studies by NASA as part of the SSP Exploratory Research and Technology (SERT) program have produced a variety of new configurations of space solar power satellites (SSPS), including the "Abacus" configuration, as described in Refs. 4 and 5. Some of these configurations, such as the "Sun Tower" configuration, are based on the passive gravity-gradient stabilization concept. However, most other configurations require three-axis attitude control to maintain continuous sun tracking of the solar arrays in the presence of external disturbances including the gravity-gradient torque. A cylindrical configuration, which is not affected by the troublesome pitch gravity-gradient torque, has also been considered by NASA.

This study focuses on the 1.2-GW geostationary Abacus satellite configuration shown in Fig. 1, characterized by its simple configuration consisting of an inertially oriented 3.2 × 3.2 km solar-array platform, a 500-m-diam microwave-beam-transmitting antenna fixed to the inertially oriented platform, and a 500 × 700 m rotating reflector that tracks the Earth. The pitch axis is nominally perpendicular to the Earth's equatorial plane (the plane of the orbit). The solar array must in fact make one rotation per year about an axis perpendicular to the orbit plane, making its attitude quasi-inertial, but this detail can be neglected in the forthcoming analysis. Some unique features of the Abacus satellite relative to the 1979 SSPS reference system are that 1) the massive transmitting antenna is not gimbaled; 2) the lightweight rotating reflector design thus eliminates massive rotary joint and slip rings of the 1979 SSPS reference system; and 3) links activated by ball–screw mechanisms can also tilt the reflector to point to ground stations at various latitudes.

In the area of dynamics and control, the overall objectives of NASA's SERT program are 1) to develop preliminary concepts for orbit, attitude, and structural control of very large SSPS using a variety of actuators such as control moment gyros, momentum wheels, and electric-propulsion thrusters; 2) to develop mathematical models, define a top-level control system architecture, and perform control system design and analysis for a baseline Abacus satellite configuration in geostationary orbit; and 3) to determine the required number, size, placement, mass, and power for the actuators to control the orbit, attitude, and structural motions of the baseline Abacus satellite.

The remainder of this paper is outlined as follows. A description of the system is provided in Sec. II, including Abacus geometry, mass distribution, orbit parameters, and control requirements. Orbital motion and the five major sources of perturbation, the most important of which is solar radiation pressure, are discussed in Sec. III. Dynamical equations of attitude motion for an inertially oriented satellite are derived in Sec. IV, and the important contributions to disturbance torque are analyzed. In Sec. V, structural control issues are briefly reviewed. Section VI describes the proposed control system architecture and provides a preliminary control design together with simulation results. Finally, a summary of major study results and recommendations for future study are presented in Sec. VII.

Received 2 December 2003; revision received 14 January 2004; accepted for publication 19 January 2004.

*Professor, Department of Mechanical and Aerospace Engineering; bong.wie@asu.edu. Associate Fellow AIAA.

†Aerospace Engineer, Spacecraft and Sensors Branch, Mail Stop 328; c.m.roithmayr@larc.nasa.gov. Senior Member AIAA.

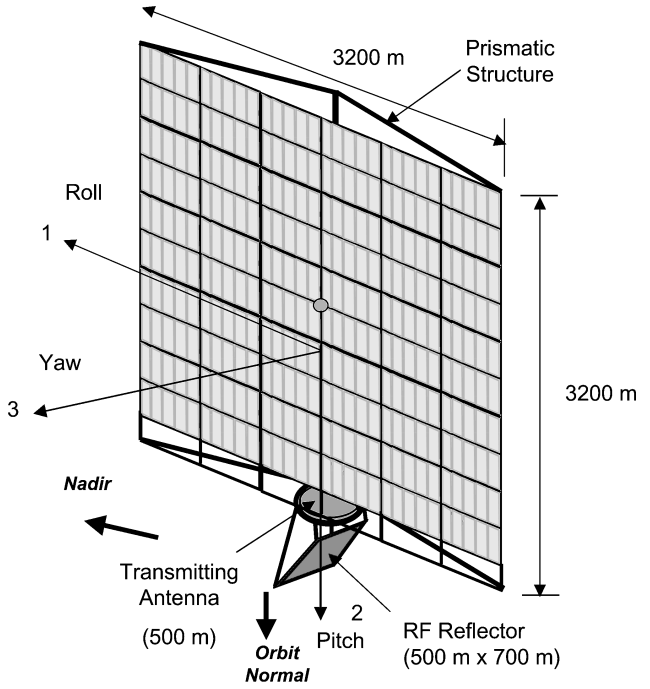

Fig. 1 Baseline 1.2-GW Abacus satellite configuration.

Table 1 Geometric and mass properties of the 1.2-GW Abacus satellite

Parameter	Value
Solar array mass	21×10^6 kg
Transmitting antenna mass	3×10^6 kg
Reflector mass	0.8×10^6 kg
Total mass	$m_B = 25 \times 10^6$ kg
Platform area	A = 3200 m × 3200 m
Area-to-mass ratio	$A/m_B = 0.4$ m^2/kg
Roll inertia	$I_1 = 2.8 \times 10^{13}$ kg · m^2
Pitch inertia	$I_2 = 1.8 \times 10^{13}$ kg · m^2
Yaw inertia	$I_3 = 4.6 \times 10^{13}$ kg · m^2
cm-cp offset	200 m (along pitch axis)
cm-cp offset (uncertainty)	±20 m (along roll axis)

Table 2 Orbit parameters and control requirements

Parameter	Value
Earth's gravitational parameter	$\mu_\oplus = 398{,}601$ km^3/s^2
Geostationary orbit	$a = 42{,}164$ km
Orbit period	23 h 56 min 4 s
Orbit rate	$n = 7.292 \times 10^{-5}$ rad/s
Stationkeeping accuracy	±0.1 deg
Eccentricity	$e < 0.0005$
Inclination	$i < 0.005$ deg
Solar array pointing accuracy	±0.5 deg for roll/pitch
Microwave beam pointing accuracy	±0.1 deg

II. System Description

A. Geometry and Mass Distribution

The Abacus satellite consists of three major parts whose dimensions are indicated in Fig. 1: an inertially oriented solar array, a transmitting antenna, and an earth-pointing reflector that moves relative to the solar array. It is important to note that the transmitting antenna is fixed to the solar array, whereas the reflector is fastened to the solar array with two rotational joints that allow the reflected microwave beam to be pointed at a particular point on the Earth's surface. The first of these is an azimuth roll-ring that permits rotation once per orbit about the solar-array pitch axis, nominally perpendicular to the Earth's equatorial plane, and the second is a set of ball–screw activated links that change the tilt of the reflector to a constant offset so that the beam can be aimed at different latitudes. This design, with a lightweight rotating reflector, eliminates the massive rotary joint and slip rings that were required for the 1979 SSPS reference system.

The total mass and area of the spacecraft are given in Table 1, together with the mass of each of the major parts. The mass of the reflector is less than 4% of the total mass; therefore, the reflector's mass and inertia can be neglected in the analysis of attitude motion, simplifying the task in two important respects. First, the Abacus satellite can be treated as a single body rather than a multibody spacecraft. When the Abacus satellite is regarded as rigid, the spacecraft's moments and products of inertia for a set of axes fixed in the solar array do not vary with time. Second, when the asymmetrical mass distribution of the reflector is left out of account, the principal axes of inertia of the spacecraft with respect to the spacecraft's mass center are parallel to the roll, pitch, and yaw axes illustrated in Fig. 1. The moments of inertia for these axes, henceforth considered to be principal moments of inertia, are given in Table 1. The center of pressure is located approximately 100 m below the geometric center of the square platform, the center of mass is located approximately 300 m below the geometric center along the pitch axis, and ±20% overall uncertainty in the mass properties is assumed in control design.

B. Orbital Parameters and Control Requirements

The general platform-attitude requirement imposed by the SERT program specifies that the pitch axis (Fig. 1) is to remain perpendicular to the Earth's equatorial plane, and the yaw axis, normal to the array, is to remain parallel to the equatorial plane. This orientation of the pitch axis is the standard, nominal attitude for all geostationary satellites with solar arrays. At the times of equinox, approximately 21 March and 21 September, the angle between the sun's rays and the orbit plane, known as the solar beta angle, will vanish; therefore, there is no power loss because the rays arrive perpendicular to the solar array. At the times of solstice, approximately 21 June and 21 December, the solar beta angle is equal to the angle between the equatorial and ecliptic planes, referred to as the obliquity of the ecliptic, with a value of 23.44 deg. On these dates power loss reaches a maximum value of only 8%, $1 - \cos(23.44\ \text{deg}) = 0.08$, which can be remedied by oversizing the array slightly, if necessary. In practice, this is how geostationary satellites accommodate power loss; the attitude of the spacecraft bus is not adjusted to compensate for variation in the solar beta angle.

On a conventional geostationary spacecraft the attitude of the solar array, sized to accommodate the seasonal power loss, is normally controlled to 0.5 deg in roll and pitch in order for solar energy to be collected. On the Abacus this requirement is superseded because the orientation of the 500 × 700 m reflector must be controlled to ±0.1 deg so that the microwave beam is aimed precisely at a point fixed to the Earth. At this time the precise performance characteristics of the rotational joints that attach the reflector to the array are unknown; therefore, in the absence of this information, we consider the precision-pointing requirements to be imposed on the array itself and pursue suitable attitude control. The design of the 500-m-diam microwave-beam-transmitting antenna and the steerable reflector and the characterization of their precision-pointing performance are of course a challenging engineering problem, but beyond the scope of this paper.

Basic orbital characteristics and control requirements for the Abacus satellite in geostationary orbit are summarized in Table 2.

III. Orbital Motion

The relative orbital motion of two bodies is governed by the second-order ordinary vector differential equation

$$\frac{{}^N\mathrm{d}^2\boldsymbol{r}}{\mathrm{d}t^2} + \frac{\mu}{r^3}\boldsymbol{r} = \boldsymbol{f} = \boldsymbol{f}_B - \boldsymbol{f}_P \tag{1}$$

where $\boldsymbol{r}$ is the position vector from the mass center $P^\star$ of a planet P to the mass center $B^\star$ of a body B, r is the magnitude of $\boldsymbol{r}$, ${}^N\mathrm{d}^2\boldsymbol{r}/\mathrm{d}t^2$ indicates the second derivative of $\boldsymbol{r}$ with respect to time t in an

inertial or Newtonian reference frame N, and $\mu \triangleq G(m_P + m_B)$, where G is the universal gravitational constant, m_P is the mass of P, and m_B is the mass of B.

If P were a sphere with uniform mass distribution, or a particle, and if B were a particle, then the gravitational force exerted by P on B would be given by $\boldsymbol{g} = -Gm_P m_B \boldsymbol{r}/r^3$. The force exerted by B on P would be simply $-\boldsymbol{g}$. The vector $\boldsymbol{f}_B$ represents the resultant force per unit mass acting on B, other than $\boldsymbol{g}/m_B$; $\boldsymbol{f}_P$ represents the resultant force per unit mass acting on P, other than $-\boldsymbol{g}/m_P$.

In the case of geostationary satellites the perturbing force per unit mass $\boldsymbol{f}$ receives significant contributions from the gravitational attraction of the sun and moon, Earth's tesseral gravitational harmonics of degree 2 and orders 0 and 2, and solar radiation pressure. The following material gives a brief development of expressions for each of these contributions, denoted respectively as $\boldsymbol{f}_s, \boldsymbol{f}_m, \boldsymbol{f}_{2,0}, \boldsymbol{f}_{2,2}$, and $\boldsymbol{f}_p$, such that

$$\boldsymbol{f} = \boldsymbol{f}_s + \boldsymbol{f}_m + \boldsymbol{f}_{2,0} + \boldsymbol{f}_{2,2} + \boldsymbol{f}_p \tag{2}$$

A. Solar and Lunar Gravitational Attraction

The gravitational force per unit mass exerted by the sun on P is given by $\mu_s \boldsymbol{r}_s / r_s^3$, where μ_s is the product of G and the sun's mass, $\boldsymbol{r}_s$ is the position vector from $P^\star$ to the sun's mass center, and r_s is the magnitude of $\boldsymbol{r}_s$. Likewise, the gravitational force per unit mass exerted by the sun on B is given by $\mu_s(\boldsymbol{r}_s - \boldsymbol{r})/|\boldsymbol{r}_s - \boldsymbol{r}|^3$. Therefore,

$$\boldsymbol{f}_s = \frac{\mu_s(\boldsymbol{r}_s - \boldsymbol{r})}{|\boldsymbol{r}_s - \boldsymbol{r}|^3} - \frac{\mu_s \boldsymbol{r}_s}{r_s^3} \tag{3}$$

When $\boldsymbol{r}$ is small in comparison to $\boldsymbol{r}_s$, numerical difficulties can be encountered in the evaluation of the right-hand member of Eq. (3); therefore, an alternate form of $\boldsymbol{f}_s$ is used, as suggested in Eq. (8.61) of Ref. 6:

$$\boldsymbol{f}_s = -\left(\mu_s \big/ |\boldsymbol{r}_s - \boldsymbol{r}|^3\right)[\boldsymbol{r} + f(q_s)\boldsymbol{r}_s] \tag{4}$$

where

$$q_s \triangleq \frac{\boldsymbol{r} \cdot (\boldsymbol{r} - 2\boldsymbol{r}_s)}{\boldsymbol{r}_s \cdot \boldsymbol{r}_s} \tag{5}$$

and the function f of q is given by

$$f(q) = q\frac{3 + 3q + q^2}{1 + (1+q)^{\frac{3}{2}}} \tag{6}$$

The contribution of lunar gravitational attraction to $\boldsymbol{f}$ is given by an expression similar to Eq. (3), and numerical difficulties are avoided with the aid of

$$\boldsymbol{f}_m = -\left(\mu_m \big/ |\boldsymbol{r}_m - \boldsymbol{r}|^3\right)[\boldsymbol{r} + f(q_m)\boldsymbol{r}_m] \tag{7}$$

where μ_m is the product of G and the moon's mass and $\boldsymbol{r}_m$ is the position vector from $P^\star$ to the moon's mass center.

B. Tesseral Harmonics

Equation (12) of Ref. 7 may be used to account for the gravitational harmonics of P, for any degree n and order m; in this study, n and m are limited to 2. Numerical values of the gravitational coefficients, gravitational parameter of Earth, and mean equatorial radius are those of the Goddard Earth Model T1 as reported in Ref. 8.

Earth's oblateness is represented by a zonal harmonic of degree 2 and order 0 and is responsible for precessions in a satellite's orbit plane and argument of perigee. The contribution of this harmonic to the force per unit mass exerted by P on B is given in Eq. (45) of Ref. 7 [also Problem 3.7(b) in Ref. 9] as

$$\boldsymbol{f}_{2,0} = -3\mu_\oplus J_2 \left(R_\oplus^2 \big/ r^4\right)\left[\sin\phi \hat{\boldsymbol{e}}_3 + \tfrac{1}{2}(1 - 5\sin^2\phi)\hat{\boldsymbol{r}}\right] \tag{8}$$

where $\mu_\oplus$ is the gravitational parameter of the Earth, the product of G and the Earth's mass; $R_\oplus$ is the mean equatorial radius of the Earth (6378.137 km); r is the magnitude of $\boldsymbol{r}$; $\hat{\boldsymbol{r}}$ is a unit vector in the direction of $\boldsymbol{r}$; and ϕ is the geocentric latitude of B. Unit vector $\hat{\boldsymbol{e}}_3$ is fixed in the Earth in the direction of the north polar axis. The zonal harmonic coefficient of degree 2 is represented by the familiar symbol J_2.

The contribution of oblateness to the force per unit mass exerted by B on P is given by $-m_B \boldsymbol{f}_{2,0}/m_P$, and the contribution of oblateness to $\boldsymbol{f}$ is thus $[1 + (m_B/m_P)]\boldsymbol{f}_{2,0}$. In the case of the Abacus orbiting Earth, $m_B = 25 \times 10^6$ kg and $m_P = 5.98 \times 10^{24}$ kg, so $m_B/m_P = 4 \times 10^{-18}$, which can be neglected in comparison to 1; therefore, the entire contribution of oblateness to $\boldsymbol{f}$ is essentially equal to $\boldsymbol{f}_{2,0}$.

The contribution $\boldsymbol{f}_{2,1}$ of the tesseral harmonic of degree 2 and order 1 vanishes because the tesseral harmonic coefficients $S_{2,1}$ and $C_{2,1}$ are both zero. The sectoral harmonic of degree 2 and order 2 can cause the longitude of a geostationary spacecraft to drift; from Eq. (12) of Ref. 7 the contribution to the force per unit mass exerted by P on B is given by

$$\begin{aligned}\boldsymbol{f}_{2,2} = \left(\mu_\oplus R_\oplus^2 \big/ r^5\right)\{&[(C_{2,2}\mathcal{C}_2 + S_{2,2}\mathcal{S}_2)/r] \\ &\times [A_{2,3}\hat{\boldsymbol{e}}_3 - (\sin\phi A_{2,3} + 5A_{2,2})\hat{\boldsymbol{r}}] \\ &+ 2A_{2,2}[(C_{2,2}\mathcal{C}_1 + S_{2,2}\mathcal{S}_1)\hat{\boldsymbol{e}}_1 + (S_{2,2}\mathcal{C}_1 - C_{2,2}\mathcal{S}_1)\hat{\boldsymbol{e}}_2]\}\end{aligned} \tag{9}$$

where unit vectors $\hat{\boldsymbol{e}}_1$ and $\hat{\boldsymbol{e}}_2$ are fixed in the Earth: $\hat{\boldsymbol{e}}_1$ lies in the equatorial plane parallel to a line intersecting Earth's geometric center and the Greenwich meridian, and $\hat{\boldsymbol{e}}_2 = \hat{\boldsymbol{e}}_3 \times \hat{\boldsymbol{e}}_1$. Sectoral harmonic coefficients of degree 2 and order 2 are denoted by $C_{2,2}$ and $S_{2,2}$.

Equations (6) and (7) of Ref. 7 indicate that the required derived Legendre polynomials are $A_{2,2} = 3$ and $A_{2,3} = 0$. In addition, Eqs. (9) and (10) of Ref. 7 show that

$$\mathcal{S}_1 = \boldsymbol{r} \cdot \hat{\boldsymbol{e}}_2 = r\cos\phi\sin\lambda, \qquad \mathcal{C}_1 = \boldsymbol{r} \cdot \hat{\boldsymbol{e}}_1 = r\cos\phi\cos\lambda \tag{10}$$

$$\mathcal{S}_2 = 2(r\cos\phi)^2\sin\lambda\cos\lambda, \qquad \mathcal{C}_2 = (r\cos\phi)^2(\cos^2\lambda - \sin^2\lambda) \tag{11}$$

where λ is the geographic longitude of B measured eastward from the Greenwich meridian. Therefore,

$$\begin{aligned}\boldsymbol{f}_{2,2} = \left(\mu_\oplus R_\oplus^2 \big/ r^4\right)\big\{&-15\cos^2\phi\big[C_{2,2}(\cos^2\lambda - \sin^2\lambda) \\ &+ 2S_{2,2}\sin\lambda\cos\lambda\big]\hat{\boldsymbol{r}} + 6\cos\phi[(C_{2,2}\cos\lambda + S_{2,2}\sin\lambda)\hat{\boldsymbol{e}}_1 \\ &+ (S_{2,2}\cos\lambda - C_{2,2}\sin\lambda)\hat{\boldsymbol{e}}_2]\big\}\end{aligned} \tag{12}$$

As far as the authors are aware, the convenient vector form of this expression is not reported elsewhere. As in the case of $\boldsymbol{f}_{2,0}$, m_B/m_P is neglected in comparison to 1, and $\boldsymbol{f}_{2,2}$ thus constitutes the entire contribution of the present harmonic to $\boldsymbol{f}$.

C. Solar Radiation Pressure

Many researchers have investigated the significant perturbation in the orbit of a large spacecraft with a large area-to-mass ratio, caused by solar radiation pressure; the orbit of the Abacus satellite (and other large SSPS) is adversely affected by an area-to-mass ratio that is very large compared to contemporary, higher-density spacecraft. A detailed physical description of the solar radiation pressure can be found in Ref. 10, a recent book on solar sailing by McInnes.

The solar-radiation-pressure forces are due to photons impinging on a surface in space, as illustrated in Fig. 2. Assuming that a fraction ρ_s of the impinging photons is specularly reflected, a fraction ρ_d is diffusely reflected, and a fraction ρ_a is absorbed by the surface, we have

$$\rho_s + \rho_d + \rho_a = 1 \tag{13}$$

The solar-radiation-pressure force $\boldsymbol{F}_p$ acting on an ideal flat surface is then expressed as in Eq. (11) on p. 262 of Ref. 11,

$$\boldsymbol{F}_p = PA(\hat{\boldsymbol{n}} \cdot \hat{\boldsymbol{s}})\left\{(\rho_a + \rho_d)\hat{\boldsymbol{s}} + \left[2\rho_s(\hat{\boldsymbol{n}} \cdot \hat{\boldsymbol{s}}) + \tfrac{2}{3}\rho_d\right]\hat{\boldsymbol{n}}\right\} \tag{14}$$

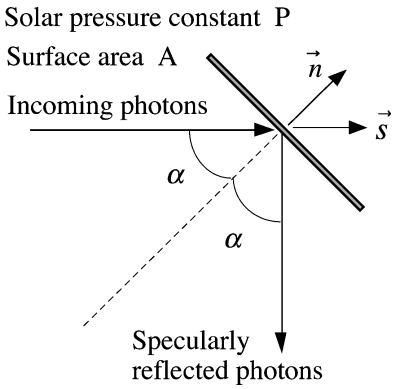

Fig. 2 Solar-radiation-pressure force acting on an ideal flat surface.

where $P = 4.5 \times 10^{-6}$ N/m^2 is the nominal solar-radiation-pressure constant, A is the surface area, $\hat{\boldsymbol{n}}$ is a unit vector normal to the surface, and $\hat{\boldsymbol{s}}$ is a unit vector having the same direction as $\boldsymbol{r} - \boldsymbol{r}_s$, the position vector from the sun's mass center to $B^\star$. The angle between $\hat{\boldsymbol{n}}$ and $\hat{\boldsymbol{s}}$ is α.

For an ideal case of a perfect mirror with $\rho_d = \rho_a = 0$, and $\rho_s = 1$, we have $\boldsymbol{F}_p = 2PA(\cos\alpha)^2\hat{\boldsymbol{n}}$. Also for an ideal case of a black body with $\rho_s = \rho_d = 0$ and $\rho_a = 1$, we have $\boldsymbol{F}_p = PA\cos\alpha\hat{\boldsymbol{s}}$. For most practical cases of satellites with a small angle of incidence α, the radiation-pressure force per unit mass exerted on B is given simply as

$$\boldsymbol{f}_p = \boldsymbol{F}_p/m_B = P(1+\rho)(A/m_B)\hat{\boldsymbol{s}} \triangleq k\hat{\boldsymbol{s}} \tag{15}$$

where ρ is the overall surface reflectance (0 for a black body and 1 for a mirror), and A/m_B is the area-to-mass ratio. The magnitude of $\boldsymbol{f}_p$ is a constant, k. We neglect the solar radiation pressure exerted on the Earth, and allow this expression to represent the total contribution of solar radiation pressure in Eq. (2).

An analytical estimate of the short-term orbital perturbations resulting from the significant in-plane component of solar radiation-pressure force is obtained as follows. First, we express $\boldsymbol{f}_p$ as

$$\boldsymbol{f}_p = f_r\hat{\boldsymbol{e}}_r + f_\theta\hat{\boldsymbol{e}}_\theta + f_z\hat{\boldsymbol{e}}_z \tag{16}$$

where unit vector $\hat{\boldsymbol{e}}_r$ is identical to $\hat{\boldsymbol{r}}$, unit vector $\hat{\boldsymbol{e}}_z$ is normal to the orbit plane and has the same direction as the specific angular momentum of $B^\star$ in N, and $\hat{\boldsymbol{e}}_r \times \hat{\boldsymbol{e}}_\theta = \hat{\boldsymbol{e}}_z$. Ignoring the effects of seasonal variations of the sun vector, $\hat{\boldsymbol{s}}$, we simply assume that $f_r \approx k\sin\theta$ and $f_\theta \approx k\cos\theta$, where θ is the true anomaly of the orbit. Although f_z is neglected for the moment, it is accounted for in detail in the numerical analysis discussed in Sec. III.D. It is well known that there is no average change over one circular orbit to the inclination i or longitude of ascending node Ω when f_z is considered constant during the orbit, a result easily shown by analytical means.

From the orbit perturbation analysis discussed in Refs. 9 and 12, the time derivatives of semimajor axis a and eccentricity e are given by

$$\frac{\mathrm{d}a}{\mathrm{d}t} = \frac{2}{n\sqrt{1-e^2}}[f_r e\sin\theta + f_\theta(1+e\cos\theta)] \tag{17a}$$

$$\frac{\mathrm{d}e}{\mathrm{d}t} = \frac{\sqrt{1-e^2}}{na}[f_r\sin\theta + f_\theta(\cos\theta + \cos E)] \tag{17b}$$

where E is the eccentric anomaly and n is the mean motion.

For geostationary satellites with a constant orbital rate of n, and $e \approx 0$, we obtain variations due to solar radiation pressure:

$$\begin{aligned}\frac{\mathrm{d}a}{\mathrm{d}t} &= \frac{2}{n}f_\theta = \frac{2k}{n}\cos\theta = \frac{2k}{n}\cos nt\\ \Rightarrow a(t) &= a(0) + \frac{2k}{n^2}\sin nt\\ \Rightarrow \Delta a &= 0 \quad \text{per day}\end{aligned} \tag{18}$$

$$\begin{aligned}\frac{\mathrm{d}e}{\mathrm{d}t} &= \frac{1}{na}(f_r\sin\theta + 2f_\theta\cos\theta)\\ &= \frac{1}{na}(k\sin^2\theta + 2k\cos^2\theta)\\ &= \frac{k}{na}\left(\frac{3}{2} + \frac{1}{2}\cos 2\theta\right)\\ \Rightarrow e(t) &= \frac{k}{na}\left(\frac{3}{2}t + \frac{1}{4n}\sin 2nt\right)\\ \Rightarrow \Delta e &\approx \frac{3\pi k}{n^2 a} \quad \text{per day}\end{aligned} \tag{19}$$

Changes in the direction of $\hat{\boldsymbol{s}}$ due to Earth's heliocentric motion should be accounted for when making long-term predictions of eccentricity growth. One such approach is described in Refs. 13 and 14. Another is presented in Ref. 15, where it is shown that eccentricity varies as $\sin^2$ over a year [Appendix A.2, Eq. (A.21)] and that the direction of the average change per orbit in the eccentricity vector is perpendicular to $\boldsymbol{r}_s$ [Eq. (3.120)].

The effect of solar radiation pressure on the change in longitude can be found by solving Hill's equations (Sec. 4.6 of Ref. 9) for in-plane motion relative to a nominal circular orbit,

$$\ddot{x} - 2n\dot{y} - 3n^2x = f_r = k\sin nt \tag{20a}$$

$$\ddot{y} + 2n\dot{x} = f_\theta = k\cos nt \tag{20b}$$

where x is the relative displacement in the radial direction, and y is the relative displacement in the direction of the velocity of the circular reference orbit. One may verify that

$$x = -(3k/2n)t\cos nt \tag{21a}$$

$$y = (k/n)[3t\sin nt + (2/n)(\cos nt - 1)] \tag{21b}$$

furnish a solution. For small angles, the longitude λ may be approximated as y/a; hence

$$\lambda(t) \approx (k/na)[3t\sin nt + (2/n)(\cos nt - 1)] \tag{22}$$

For the Abacus satellite with an area-to-mass ratio $A/m_B \approx 0.4$ m^2/kg, assuming an overall surface reflectance $\rho = 0.3$, we have

$$F_p = (4.5\times10^{-6})(1.3)(10.24\times10^6) \approx 60\,\text{N}$$

$$k = F_p/m_B \approx 2.4\times10^{-6}\ \text{m/s}^2$$

$$\Delta e = 3\pi k/(n^2 a) \approx 1\times10^{-4} \quad \text{per day}$$

In view of Eq. (22), or Eq. (3.123) of Ref. 15, the longitude drift is given as $\Delta\lambda = 2\Delta e \approx 0.0115$ deg/day. Thus the stationkeeping requirement of 0.1 deg set forth in Table 2 is exceeded after less than 10 days of uncontrolled eccentricity growth. The well-known sun-pointing-perigee technique of directing the eccentricity vector toward the sun, discussed in Ref. 14, is used to control eccentricity growth of typical geosynchronous satellites; however, this approach may not be applicable to the Abacus with a stationkeeping requirement of 0.1 deg in the presence of a large area-to-mass ratio of 0.4 m^2/kg. Use of this strategy is also questionable in light of the need for continuous cancellation of gravitational moment for attitude control as discussed in the next section. Consequently, continuous orbit-eccentricity control using high-specific-impulse (I_{sp}) ion engines becomes attractive.

D. Simulation Results

Orbital motion of the Abacus satellite is simulated by solving Eqs. (1) with Encke's method, as described in Sec. 9.4 of Ref. 6 and 9.3 of Ref. 16. The right-hand member of Eqs. (1) is given by Eq. (2) and evaluated by means of Eqs. (4), (7), (8), (12), and (15),

which account in detail for all components of perturbing force per unit mass.

The initial values used in the simulations correspond to a circular, equatorial orbit of radius 42,164.169 km; therefore, the initial orbital elements are $a = 42{,}164.169$ km and $e = i = \Omega = \omega = 0$. The epoch used to calculate the solar and lunar positions, as well as the Earth's orientation in inertial space, according to formulas given in Ref. 17, is 21 June 2000. On this date $\boldsymbol{r}_s$ is approximately 90 deg ahead of the vernal-equinox direction in the ecliptic plane. To place the spacecraft at an initial terrestrial longitude of 75.07 deg (one of the stable longitudes), a true anomaly θ of -15.43 deg is used. These elements correspond to an initial position and velocity of

$$\boldsymbol{r} = X\hat{\boldsymbol{I}} + Y\hat{\boldsymbol{J}} + Z\hat{\boldsymbol{K}} = 40{,}644.757\,\hat{\boldsymbol{I}} - 11{,}216.990\,\hat{\boldsymbol{J}}\ (\text{km})$$

$$\boldsymbol{v} = 0.818\,\hat{\boldsymbol{I}} + 2.964\,\hat{\boldsymbol{J}}\ (\text{km/s})$$

where $\hat{\boldsymbol{I}}$, $\hat{\boldsymbol{J}}$, and $\hat{\boldsymbol{K}}$ make up a set of unit vectors fixed in an Earth-centered-inertial reference frame.

Solution of the requisite six scalar first-order ordinary differential equations is obtained by numerical integration with a variable-step Runge–Kutta scheme, with relative and absolute error tolerances set to 1×10^{-8}. The true position and velocity are computed and used to determine values of classical orbital elements.

The results of a 30-day simulation of uncontrolled orbital motion, including the effects of Earth's oblateness and triaxiality, lunisolar perturbations, and a 60-N solar-pressure force, are shown in Fig. 3. The 30-day secular growth in eccentricity of 3×10^{-3} confirms the conclusion reached in Sec. III.C that solar radiation pressure must be offset if stationkeeping requirements are to be met. The average slope of inclination in Fig. 3 is about 0.0783 deg/month, corresponding to a yearly growth of 0.940 deg; this is caused by the solar and lunar gravitational perturbations expressed in Eqs. (4) and (7) and is within the expected range given on p. 82 of Ref. 12.

In the next section we develop a dynamic model of attitude motion of an inertially oriented spacecraft in geostationary orbit, in preparation for the design of an attitude control system.

IV. Attitude Motion of an Inertially Oriented Spacecraft

Euler's equations for rotational motion of a rigid body B can be expressed in vector–dyadic form as

$$\underline{\boldsymbol{I}} \cdot {}^N\boldsymbol{\alpha}^B + {}^N\boldsymbol{\omega}^B \times \underline{\boldsymbol{I}} \cdot {}^N\boldsymbol{\omega}^B = \boldsymbol{\tau} = \boldsymbol{M} + \boldsymbol{u} + \boldsymbol{d} \tag{23}$$

where $\underline{\boldsymbol{I}}$ is the inertia dyadic of B with respect to its mass center $B^\star$, ${}^N\boldsymbol{\omega}^B$ is the angular velocity of B in an inertial or Newtonian reference frame N, and ${}^N\boldsymbol{\alpha}^B$ is the angular acceleration of B in N, ${}^N\boldsymbol{\alpha}^B \triangleq {}^N\mathrm{d}{}^N\boldsymbol{\omega}^B/\mathrm{d}t = {}^B\mathrm{d}{}^N\boldsymbol{\omega}^B/\mathrm{d}t$, with ${}^N\mathrm{d}/\mathrm{d}t$ and ${}^B\mathrm{d}/\mathrm{d}t$ denoting differentiation with respect to time in N and in B, respectively. The vector $\boldsymbol{\tau}$ represents the moment about $B^\star$ of external forces acting on B and is regarded as the sum of the gravitational moment $\boldsymbol{M}$ exerted by the primary P, the moment $\boldsymbol{u}$ exerted by control actuators, and the remaining contributions $\boldsymbol{d}$.

The gravitational moment exerted by P is often calculated by neglecting its gravitational harmonics and treating it as a particle, or a sphere with uniform mass distribution, in which case $\boldsymbol{M}$, also known as gravity-gradient torque, can be expressed according to Refs. 9 and 18:

$$\boldsymbol{M} = 3\left(\mu_\oplus \big/ r^3\right)\hat{\boldsymbol{r}} \times \underline{\boldsymbol{I}} \cdot \hat{\boldsymbol{r}} \tag{24}$$

where $\hat{\boldsymbol{r}}$ is a unit vector having the same direction as the position vector from $P^\star$ to $B^\star$.

It is convenient to work with a set of right-handed, mutually perpendicular unit vectors $\hat{\boldsymbol{b}}_1$, $\hat{\boldsymbol{b}}_2$, and $\hat{\boldsymbol{b}}_3$ fixed in B and introduce the dot products

$$\omega_i \triangleq {}^N\boldsymbol{\omega}^B \cdot \hat{\boldsymbol{b}}_i, \qquad r_i \triangleq \hat{\boldsymbol{r}} \cdot \hat{\boldsymbol{b}}_i, \qquad u_i \triangleq \boldsymbol{u} \cdot \hat{\boldsymbol{b}}_i, \qquad d_i \triangleq \boldsymbol{d} \cdot \hat{\boldsymbol{b}}_i \quad (i = 1, 2, 3) \tag{25}$$

If $\hat{\boldsymbol{b}}_1$, $\hat{\boldsymbol{b}}_2$, and $\hat{\boldsymbol{b}}_3$ are taken to be parallel to central principal axes of inertia of B, then the central principal moments of inertia of B can be expressed as

$$I_i \triangleq \hat{\boldsymbol{b}}_i \cdot \underline{\boldsymbol{I}} \cdot \hat{\boldsymbol{b}}_i \qquad (i = 1, 2, 3) \tag{26}$$

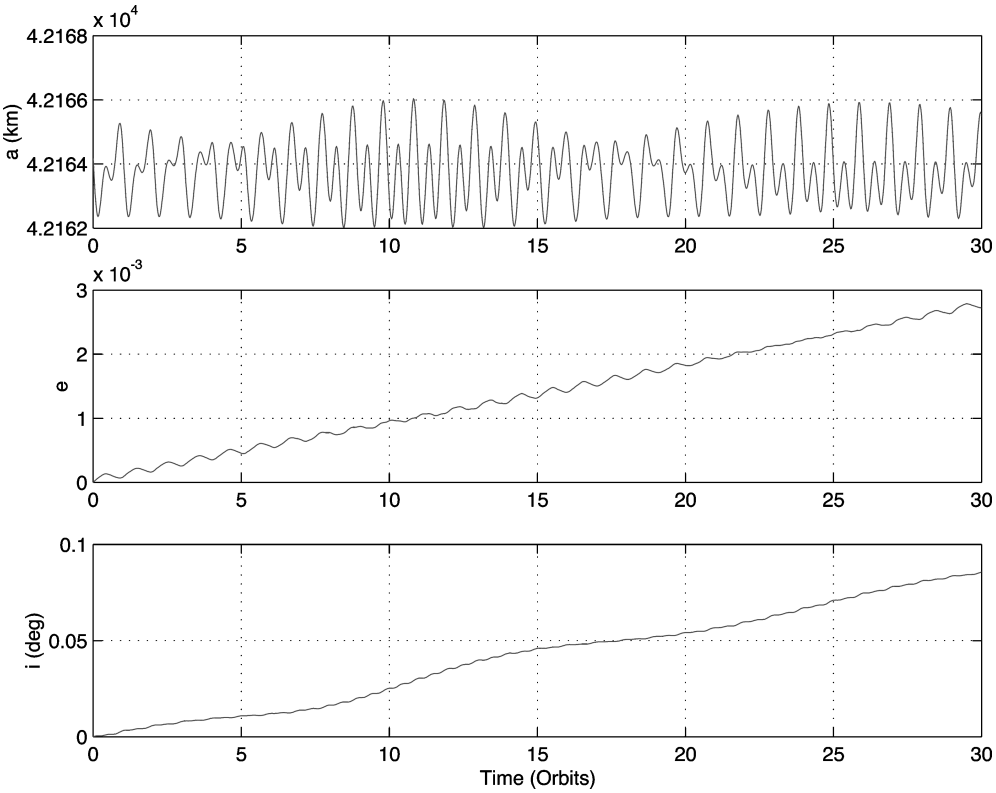

Fig. 3 Orbit simulation results of the Abacus satellite with the effects of the Earth's oblateness and triaxiality, lunisolar perturbations, and 60-N solar-radiation-pressure force.

If it is assumed that B travels in a circular orbit with constant orbital rate n given by $\sqrt{(\mu_\oplus/r^3)}$, the nonlinear equations (23) can be expressed in scalar form as

$$I_1\dot{\omega}_1 + (I_3 - I_2)\omega_2\omega_3 = 3n^2(I_3 - I_2)r_2r_3 + u_1 + d_1 \quad (27a)$$

$$I_2\dot{\omega}_2 + (I_1 - I_3)\omega_3\omega_1 = 3n^2(I_1 - I_3)r_3r_1 + u_2 + d_2 \quad (27b)$$

$$I_3\dot{\omega}_3 + (I_2 - I_1)\omega_1\omega_2 = 3n^2(I_2 - I_1)r_1r_2 + u_3 + d_3 \quad (27c)$$

Because Abacus is regarded here as a single body B whose nominal orientation is fixed in an inertial reference frame N, we introduce three unit vectors $\hat{\boldsymbol{n}}_1$, $\hat{\boldsymbol{n}}_2$, and $\hat{\boldsymbol{n}}_3$ fixed in N such that Earth's equatorial plane contains $\hat{\boldsymbol{n}}_1$ and $\hat{\boldsymbol{n}}_3$, whereas $\hat{\boldsymbol{n}}_2$ is perpendicular to the equatorial plane. To describe the orientation of B in N, we choose a pitch–yaw–roll sequence described as follows. With $\hat{\boldsymbol{b}}_i$ having the same direction as $\hat{\boldsymbol{n}}_i (i = 1, 2, 3)$, proceed with a rotation first about $\hat{\boldsymbol{b}}_2$ in the amount θ_2, followed by a rotation about $\hat{\boldsymbol{b}}_3$ in the amount θ_3, and conclude with a rotation about $\hat{\boldsymbol{b}}_1$ in the amount θ_1. For this rotational sequence, we have

$$\begin{bmatrix} \hat{\boldsymbol{b}}_1 \\ \hat{\boldsymbol{b}}_2 \\ \hat{\boldsymbol{b}}_3 \end{bmatrix} = \begin{bmatrix} C_2C_3 & S_3 & -S_2C_3 \\ -C_2S_3C_1 + S_1S_2 & C_3C_1 & S_2S_3C_1 + S_1C_2 \\ C_2S_3S_1 + C_1S_2 & -C_3S_1 & -S_2S_3S_1 + C_1C_2 \end{bmatrix} \begin{bmatrix} \hat{\boldsymbol{n}}_1 \\ \hat{\boldsymbol{n}}_2 \\ \hat{\boldsymbol{n}}_3 \end{bmatrix} \quad (28)$$

where $C_1 \triangleq \cos\theta_1$, $S_2 \triangleq \sin\theta_2$, etc.

The unit vector $\hat{\boldsymbol{r}}$ can be expressed as

$$\hat{\boldsymbol{r}} = \cos nt\,\hat{\boldsymbol{n}}_3 - \sin nt\,\hat{\boldsymbol{n}}_1 \quad (29)$$

in which case

$$r_1 = -S_2C_3\cos nt - C_2C_3\sin nt \quad (30a)$$

$$r_2 = (S_2S_3C_1 + S_1C_2)\cos nt - (-C_2S_3C_1 + S_1S_2)\sin nt \quad (30b)$$

$$r_3 = (-S_2S_3S_1 + C_1C_2)\cos nt - (C_2S_3S_1 + C_1S_2)\sin nt \quad (30c)$$

It is clear that Eqs. (27) and (30) are nonlinear in ω_i and θ_i, variables that may take on arbitrarily large values in the general case. However, ω_i and θ_i would all be zero if the attitude motion of the Abacus were controlled as intended. (The yearly rotation of the solar array about an axis perpendicular to the orbit plane is neglected.) Thus, we introduce quantities that are assumed to remain small, denoted with a tilde:

$$\omega_i = 0 + \tilde{\omega}_i, \qquad \theta_i = 0 + \tilde{\theta}_i \qquad (i = 1, 2, 3) \quad (31)$$

It is easily shown that, expressed in terms of these quantities, the kinematical differential equations for the orientation angles are simply

$$\dot{\tilde{\theta}}_i \approx \tilde{\omega}_i \qquad (i = 1, 2, 3) \quad (32)$$

After substitution from Eqs. (30) into Eqs. (27), expansion of trigonometric functions into power series, substitution from Eqs. (31) and (32), and omission of all terms of second or higher degree in the quantities assumed to be small, the dynamical equations linearized about the nominal motion are written as

$$I_1\ddot{\tilde{\theta}}_1 = 3n^2(I_3 - I_2)\left[(\cos^2 nt)\tilde{\theta}_1 + (\sin nt\cos nt)\tilde{\theta}_3\right] + u_1 + d_1 \quad (33a)$$

$$I_2\ddot{\tilde{\theta}}_2 = 3n^2(I_3 - I_1)\left[(\cos^2 nt - \sin^2 nt)\tilde{\theta}_2 + \sin nt\cos nt\right] + u_2 + d_2 \quad (33b)$$

$$I_3\ddot{\tilde{\theta}}_3 = 3n^2(I_1 - I_2)\left[(\sin^2 nt)\tilde{\theta}_3 + (\sin nt\cos nt)\tilde{\theta}_1\right] + u_3 + d_3 \quad (33c)$$

Equations (33) are the attitude equations of motion of the Abacus satellite for control design. It can be seen that the pitch motion is decoupled from the roll/yaw motion, but the pitching motion is significantly disturbed by the time-varying gravity-gradient torque. Various ways of dealing with this issue are discussed in Sec. IV.A. Furthermore, the roll/yaw motion is strongly coupled due to the time-varying roll/yaw gravity-gradient torques. The other external disturbances d_i are developed presently in Sec. IV.B.

A. Pitch Gravity Gradient Torque and Momentum

In the absence of any pitch attitude error $\tilde{\theta}_2 = 0$, and the pitch equation of motion for an inertially oriented spacecraft in circular orbit, Eq. (33b), can be rewritten as

$$I_2\ddot{\tilde{\theta}}_2 = (3n^2/2)(I_3 - I_1)\sin 2nt + u_2 + d_2 \quad (34)$$

Ignoring for the moment any other disturbance d_2, the pitch-control torque u_2 required to counter the cyclic gravity-gradient torque becomes simply

$$u_2 = -(3n^2/2)(I_3 - I_1)\sin 2nt \quad (35)$$

with peak values of $\pm 143{,}000\ \mathrm{N\cdot m}$.

If angular-momentum-exchange devices, such as momentum wheels or control moment gyros (CMGs), are to be employed for pitch control, the peak angular momentum to be stored can then be estimated as

$$H_{\max} = (3n/2)(I_3 - I_1) = 2 \times 10^9\ \mathrm{N\cdot m\cdot s} \quad (36)$$

This is about 100,000 times the angular momentum storage requirement of the International Space Station (ISS), which is controlled by four double-gimbaled CMGs with a total momentum storage capability of about $20{,}000\ \mathrm{N\cdot m\cdot s}$ and a momentum density of $17.5\ \mathrm{N\cdot m\cdot s/kg}$. Basic characteristics of a large single-gimbal CMG are summarized in Table 3; these devices have a momentum density of $28\ \mathrm{N\cdot m\cdot s/kg}$. Future advanced flywheels may have a larger momentum density of $150\ \mathrm{N\cdot m\cdot s/kg}$. In view of all of this, it can be concluded that a traditional momentum management approach employing conventional CMGs (or even future advanced flywheels) is not a viable option for controlling a very large SSPS.

To meet the momentum storage requirement of very large SSPS, a concept of constructing large-diameter momentum wheels in space was proposed in the late 1970s in Ref. 19. In an attempt to resolve the angular-momentum storage problem of large sun-pointing spacecraft, a quasi-inertial sun-pointing pitch-control concept was developed by Elrod in 1972 and reported in Ref. 20, and further investigated by Juang and Wang in 1982 as described in Ref. 21. However, such a "free-drift" concept is not a viable option for the Abacus satellite because of the large pitch-attitude peak error of 18.8 deg and the inherent sensitivity with respect to initial phasing and other orbital perturbations.

Because the pitch gravity-gradient torque becomes naturally zero for cylindrical, spherical, or beamlike satellites with $I_1 = I_3$, a cylindrical SSPS configuration (see Fig. 1.2, Ref. 22) was also studied by NASA as a simple way to avoid such a troublesome pitch gravity-gradient torque problem.

Table 3 A large single-gimbal CMG (courtesy of Honeywell Space Systems, Glendale, Arizona)

Parameter	Value
Cost	\$1M
Momentum	$7000\ \mathrm{N\cdot m\cdot s}$
Max torque	$4000\ \mathrm{N\cdot m}$
Peak power	500 W
Mass	250 kg
Momentum/mass	$28\ \mathrm{N\cdot m\cdot s/kg}$

Table 4 Solar pressure and microwave radiation disturbances

Parameter	Value
Solar pressure force	$(4.5 \times 10^{-6})(1.3)(\text{A}) = 60$ N
Solar pressure torque (roll)	60 N × 200 m
Solar pressure torque (pitch)	60 N × 20 m
Reflector radiation force	7 N (rotating force)
Reflector radiation torque	7 N × 1700 m

B. Microwave and Solar-Radiation-Pressure Torques

The remaining contributions to disturbance torque come from solar-radiation-pressure force $\boldsymbol{F}_p$ applied at the center of pressure, as discussed in Sec. III.C, and a force applied at the center of the microwave reflector in reaction to the discharge of the microwave beam. These disturbances, with ±20% overall uncertainty, are summarized in Table 4. Disturbance torque in units of N · m, due to solar pressure, microwave radiation, cm-cp offset, and cm-cp offset uncertainty, can be expressed along the platform-fixed control axes as

$$d_1 \approx 12{,}000 - 11{,}900\cos nt \quad \text{(roll)} \tag{37a}$$

$$d_2 \approx 1200 \quad \text{(pitch)} \tag{37b}$$

$$d_3 \approx -11{,}900\sin nt \quad \text{(yaw)} \tag{37c}$$

The constant pitch-disturbance torque of 1200 N · m is small in comparison to the sinusoidal gravity-gradient torque and is due to the assumed cm-cp offset of 20 m along the roll axis; ±20% uncertainty in this disturbance model is assumed in control design.

It is assumed that the electric currents circulate in the solar-array structure in such a way that magnetic fields cancel out, and the Abacus satellite is not affected by the magnetic field of the Earth.

V. Structural Control Issues

A significant problem with control–structure interaction is quite naturally a major concern in connection with a very large platform such as the 3.2 × 3.2 km Abacus, whose lowest structural mode has a frequency of about 0.002 Hz. Dynamics and control of similar large flexible structures have been investigated by many researchers in the past (see, for example, Refs. 23–25), and active structural-vibration control is a topic of continuing practical as well as theoretical interest.

The best way of dealing with such a problem is to avoid the conditions under which it occurs in the first place, an objective accomplished simply by employing a control bandwidth lower than 1×10^{-5} Hz in the systems that control the orbit and attitude. This is not to say that structural control of the Abacus is completely unnecessary, but the focus of this paper is the preliminary design of a system for controlling the orbit and attitude without exciting structural vibrations. Although the problem of active structural control is not studied further in what follows, additional investigation of possible structural-dynamic interaction between the transmitter and reflector in the Abacus configuration is certainly advised. Various structural concepts for providing the required stiffness and rigidity of the Abacus platform are illustrated in Fig. 2.12 of Ref. 22.

A low-bandwidth attitude control system is proposed in the following section; a concept of cyclic-disturbance accommodation control is utilized to provide the required ±0.1 deg pointing accuracy in the presence of large, but slowly varying, external disturbances and dynamic modeling uncertainties.

VI. Attitude and Orbit Control

As demonstrated in Sec. III.C, solar radiation pressure, if left unopposed, could cause a drift in the longitude of the Abacus of 0.3 deg per month, east or west. Current geosynchronous satellite control systems are perfectly capable of meeting a north–south and east–west stationkeeping requirement of ±0.1 deg and would suffice for the Abacus were it not for the unusually large perturbation from solar radiation pressure. To the extent that this perturbation can be eliminated through the use of thrusters, the major difference between the Abacus and current geosynchronous spacecraft vanishes, and the problem of stationkeeping is reduced to one that has already been solved. Hence, we concentrate in what follows on using ion thrusters with high specific impulse to control the secular growth in eccentricity and inclination exhibited in Fig. 3, rather than on design and performance of a traditional stationkeeping control system.

As discussed in Secs. IV.A and IV.B, continuous sun tracking by the Abacus satellite requires large control torques to counter various disturbance torques. Thus, the control system architecture developed in this study utilizes properly distributed and oriented ion thrusters to negate the solar-radiation-pressure force; by applying this thrust in a cyclic fashion, the cyclic pitch gravity-gradient torque is opposed at the same time. Consequently, roll and pitch attitude control require no additional expenditure of fuel over and above what is already required for orbit maintenance.

A. Electric Propulsion System

In principle, an electric propulsion system employs electrical energy to accelerate ionized particles to extremely high velocities, giving a large total impulse for a small consumption of propellant. In contrast to standard propulsion, in which the products of chemical combustion are expelled from a rocket engine, ion propulsion is accomplished by giving a gas, such as xenon (which is like neon or helium, but heavier), an electrical charge and electrically accelerating the ionized gas to a speed of about 30 km/s. When xenon ions are emitted at such high speed as exhaust from a spacecraft, they push the spacecraft in the opposite direction. Basic characteristics of an electric propulsion system for the Abacus satellite are summarized in Table 5.

The amount of propellant required for typical north–south and east–west stationkeeping maneuvers for the Abacus satellite is estimated as

$$\Delta m = m_B\{1 - \exp[-\Delta V/(g I_{\text{sp}})]\} \approx 30{,}000 \text{ kg/year}$$

where $m_B = 25 \times 10^6$ kg, $\Delta V = 50$ m/s per year (Table 2.4, Ref. 12, or p. 106, Ref. 14), $g = 9.8$ m/s^2, and $I_{\text{sp}} = 5000$ s. An estimate for the yearly propellant requirement to counter the solar-pressure force of approximately 60 N is given by

$$\Delta m = \frac{(60)(24 \times 3600 \times 365)}{5000 \times 9.8} \approx 40{,}000 \text{ kg/year}$$

and is associated with a ΔV of 76 m/s per year. Including 15,000 kg of reserve propellant, the estimated total yearly propellant consumption for orbit maintenance alone is 85,000 kg when electric-propulsion thrusters that have an I_{sp} of 5000 s are used. Even though this amount of propellant is larger than the current annual worldwide production of xenon, about 40,000 kg, it must be remembered that the spacecraft has a total mass of 25×10^6 kg, and so the yearly stationkeeping propellant load is not at all unreasonable. If a way is found to construct a 3.2 × 3.2 km array, then supplying 85,000 kg

Table 5 Electric propulsion system for the 1.2-GW Abacus satellite

Parameter[a]	Value
Thrust T	≥1 N
Specific impulse $I_{\text{sp}} = T/(\dot{m}g)$	≥5000 s
Exhaust velocity $V_e = I_{\text{sp}}g$	≥49 km/s
Total efficiency $\eta = P_o/P_i$	≥80%
Power/thrust ratio P_i/T	≤30 kW/N
Mass/power ratio	≤5 kg/kW
Total peak thrust	200 N
Total peak power	6 MW
Total average thrust	80 N
Total average power	2.4 MW
Number of 1-N thrusters	≥500
Total dry mass	≥75,000 kg
Propellant consumption	85,000 kg/year

[a] $T = \dot{m}V_e$, $P_o = \frac{1}{2}\dot{m}V_e^2 = \frac{1}{2}TV_e$, $P_o/T = \frac{1}{2}V_e$ = ideal power/thrust ratio, $P_i/T = (1/2\eta)V_e$, $I_{\text{sp}} = T/(\dot{m}g) = V_e/g$, $V_e = I_{\text{sp}}g$, where $g = 9.8$ m/s^2, $\dot{m}$ is the exhaust mass flow rate, P_i is the input power, and P_o is the output power.

of propellant each year and using 500 thrusters can certainly be considered practical. The yearly propellant requirement is reduced to 21,000 kg if an I_{sp} of 20,000 s can be achieved (as was assumed for the 1979 SSPS reference system). As I_{sp} is increased, the propellant mass decreases but the electric power requirement increases; consequently, the mass of solar arrays and power processing units increases. Based on a minimum of 500 1-N thrusters, a mass/power ratio of 5 kg/kW, and a power/thrust ratio of 30 kW/N, the total dry mass (power processing units, thrusters, tanks, feed systems, etc.) of an electric propulsion system proposed for the Abacus satellite is estimated as 75,000 kg.

The capability of present electric thrusters is orders of magnitude below that required for the Abacus satellite. If the xenon-fueled, 1-kW level, off-the-shelf ion engines available today are to be employed, the number of thrusters would be increased to 15,000. The actual total number of ion engines will further increase significantly when we consider the ion engine's lifetime, reliability, duty cycle, and redundancy.

For example, the 2.3-kW, 30-cm-diam ion engine of the Deep Space 1 spacecraft has a maximum thrust level of 92 mN. Throttling down is achieved by reducing the voltage and the amount of xenon propellant injected into the engine. Specific impulse ranges from 1900 s at the minimum throttle level to 3200 s.

B. Preliminary Control System Design

A proposed preliminary control system architecture, shown in Fig. 4, utilizes properly distributed and oriented ion thrusters to counteract the solar-radiation-pressure force whose average value is about 60 N. The same thrusters are used to counter the secular roll torque caused by an offset of the center of mass and center of pressure; furthermore, the thrusters are employed in a cyclic fashion to oppose the cyclic pitch gravity-gradient and roll/yaw microwave-radiation torques.

It is assumed that three-axis inertial-attitude information in terms of quaternions will be available from an attitude determination subsystem, consisting of sun sensors, star camera/trackers, and inertial-measurement units (IMUs). The IMUs contain rate gyros, and they are critical components of a spacecraft attitude determination subsystem.

The significant control–structure interaction problem, which is a major concern for such a very large Abacus platform with the lowest structural mode frequency of 0.002 Hz, is simply avoided by designing an attitude control system with very low bandwidth (<orbit frequency). Because the lowest "dominant" flexible-mode frequency of the Abacus platform is about 0.02 Hz, all structural modes are gain-stabilized by a large spectral separation between the rigid-body control and dominant flexible modes. A major drawback of such a low-bandwidth attitude control system is its low pointing performance in the presence of persistent disturbances.

However, the proposed low-bandwidth attitude control system utilizes a concept of cyclic-disturbance accommodating control to provide ±0.1 deg pointing in the presence of large, but slowly varying, external disturbances and dynamic modeling uncertainties. The concept of cyclic-disturbance accommodation control has been successfully applied to a variety of space vehicle control problems, including the Hubble Space Telescope,[26] the International Space Station,[27,28] and flexible space structures.[29–31] Detailed technical discussions of practical control system design for space vehicles in the presence of structural flexibility, as well as persistent external disturbances, can be found in Refs. 9 and 26–31. Thus, theoretical aspects of the control-law design problem of the Abacus satellite are not elaborated upon in this paper. Even though the need for structural control is by and large eliminated by gain stabilization, it is of course prudent to anticipate the use of high-bandwidth collocated-direct-velocity-feedback active dampers, properly distributed over

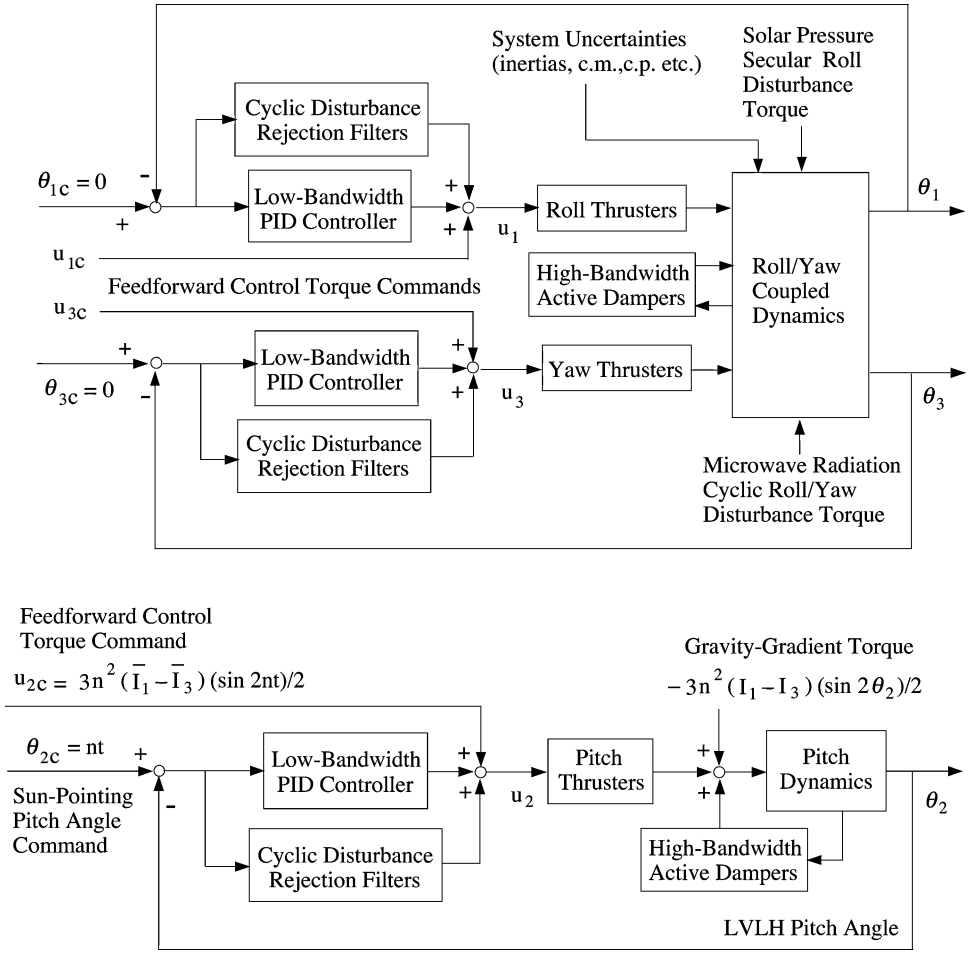

Fig. 4 Proposed attitude-control-system architecture employing electric propulsion thrusters.

the platform. Detailed design and analysis of damper performance has not been performed, although this should be undertaken in the future; therefore, Fig. 4 reflects the possible use of active dampers.

Although the roll/yaw motions are strongly coupled, a feedforward decoupling control approach provides a practical way of avoiding a time-varying, multivariable control design. A constant-gain, decoupled controller is designed for the following desired closed-loop poles (in units of the orbital rate, n) for each axis:

$$\text{PID attitude controller: } -0.5 \pm 0.5j, \qquad -0.2$$

$$\text{cyclic-disturbance rejection filters: } -0.2 \pm j, \qquad -0.2 \pm 2j$$

For a standard PID control design, the integral control gain (or equivalently, the real eigenvalue associated with the integral control) is chosen as discussed on p. 125 of Ref. 9.

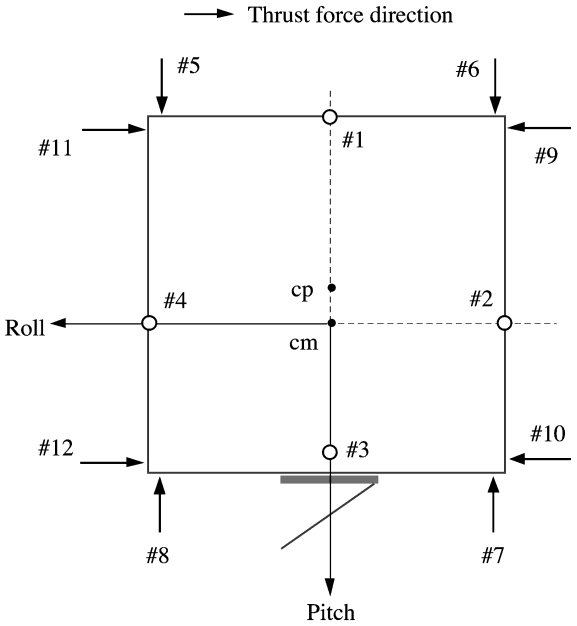

Fig. 5 Placement of a minimum of 500 1-N electric propulsion thrusters at 12 different locations, with 100 thrusters each at locations 2 and 4.

Placement of approximately 500 1-N electric-propulsion thrusters at 12 different locations is illustrated in Fig. 5. In contrast to a typical placement of thrusters at the four corners, e.g., employed for the 1979 SSPS reference system, the proposed placement shown in Fig. 5 minimizes roll/pitch thruster couplings as well as the excitation of platform out-of-plane structural modes. Thrusters 2 and 4 are 1600 m from the center of mass; therefore, approximately 90 N of thrust must be applied at one of these locations in order to counteract a gravitational moment of 143,000 N · m as indicated in Eq. (35). A sinusoidal moment can be exerted if, for example, 1-N thrusters are used and 100 thrusters (to be conservative) are placed at each of locations 2 and 4. Likewise, approximately 15 1-N thrusters are required to offset the maximum roll torque from Eq. (37a), and a conservative number of 30 1-N thrusters is placed at each of the 10 locations 1, 3, and 5–12. Consequently, a minimum of 500 ion engines of 1-N thrust level are required for simultaneous attitude and orbit control. When reliability, lifetime, duty cycle, lower thrust level, and redundancy of ion engines are considered, this number will increase significantly.

Thrusters 1 and 3, which control roll attitude, and thrusters 2 and 4, which control pitch, all apply thrust in the positive yaw direction; that is, the thrust is directed toward the side of the array that faces the sun. With this arrangement, a cyclic pitch-control torque is produced through the alternate use of thrusters 2 and 4; no matter which one is used, a force is produced perpendicular to the array and thus the largest component of solar-radiation-pressure force is opposed at the same time that pitch attitude is controlled. Likewise, roll control also contributes to elimination of the solar-radiation-pressure force. During those times of the year when there is a component of solar-radiation-pressure force perpendicular to the equatorial (orbit) plane, thrusters 5–8 can be used to cancel it. Thus, the propellant

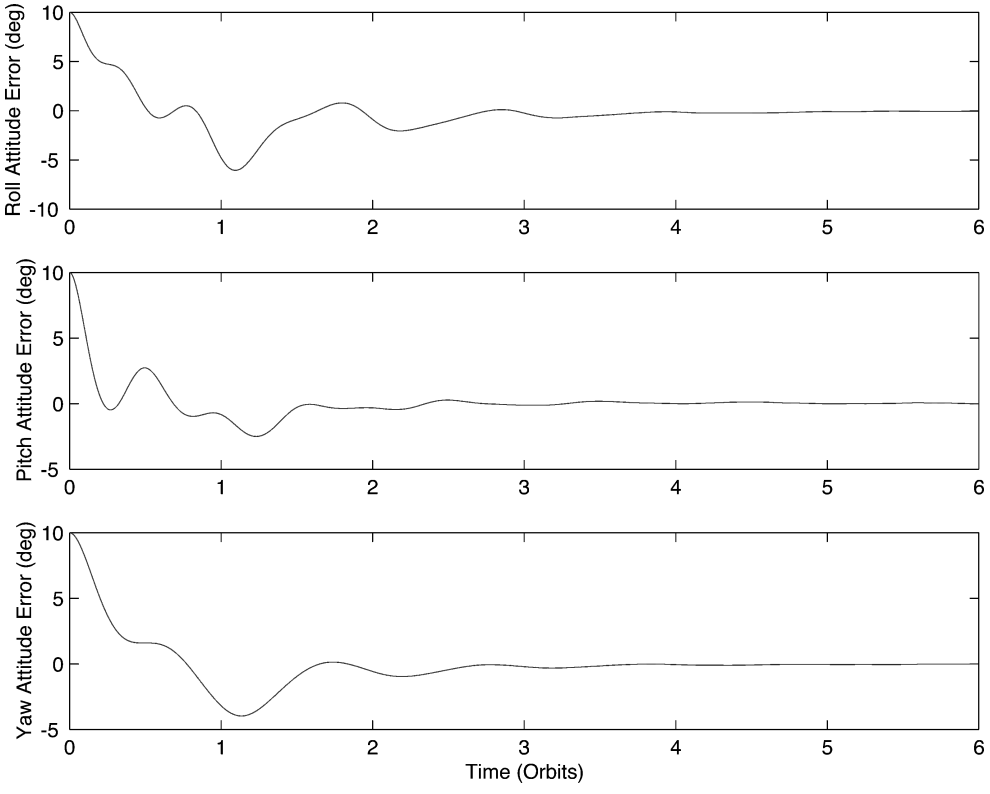

Fig. 6 Rigid-body-control simulation results for the proposed attitude-control-system architecture.

needed solely for orbit control is applied in such a way that attitude control is accomplished essentially at no cost.

C. Simulation Results

Attitude-control-system simulation results from an illustrative case involving a single rigid-body model, with 10-deg initial attitude errors in each axis, are shown in Figs. 6–9. Control gains are produced with the values given in Table 1 for the principal moments of inertia and cm-cp offset; however, the simulation is carried out with values that differ by ±20% in order to introduce intentional dynamic modeling errors. No active dampers were included for this simulation study. As can be seen in Fig. 7, the proposed low-bandwidth attitude control system, which effectively utilizes the concept of cyclic-disturbance accommodation control, maintains the required steady-state pointing of the Abacus platform in the presence of large, but slowly varying,

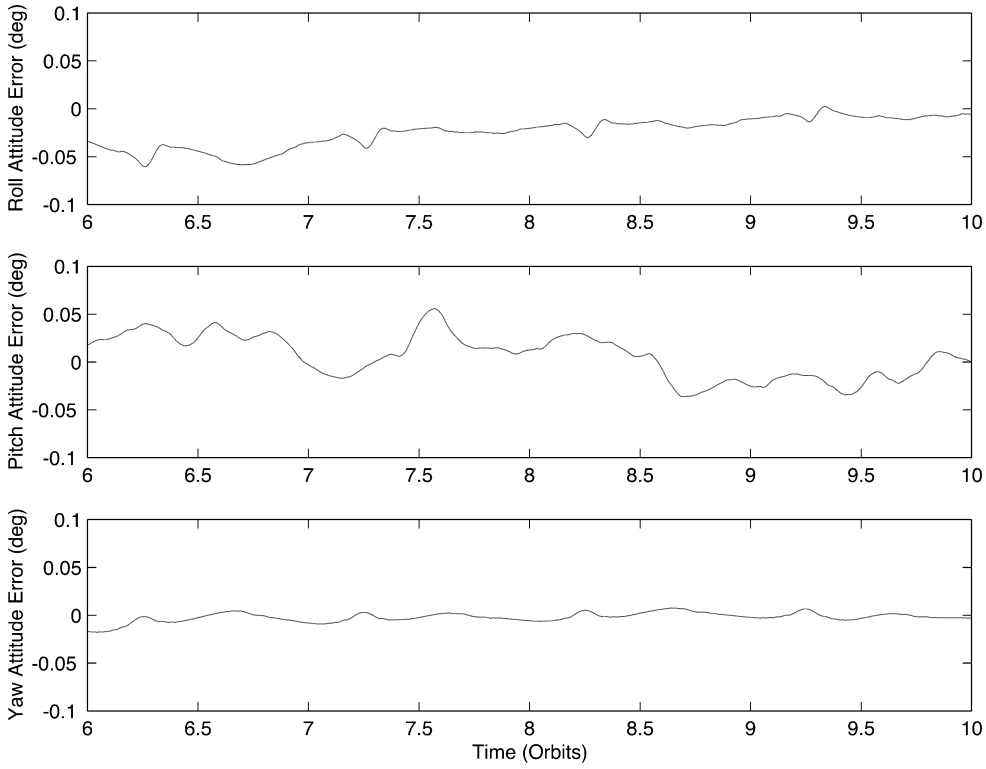

Fig. 7 Rigid-body-control simulation results for demonstrating the steady-state pointing performance of meeting the 0.1-deg pointing requirement.

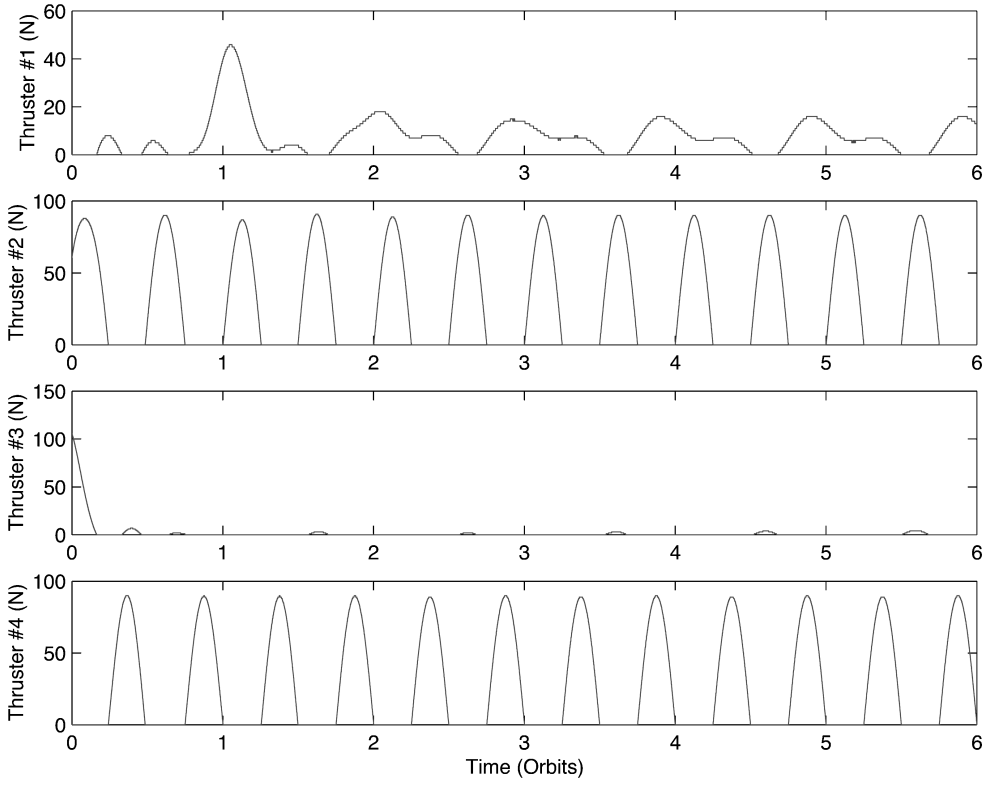

Fig. 8 Rigid-body-control simulation results for the proposed attitude-control-system architecture (continued).

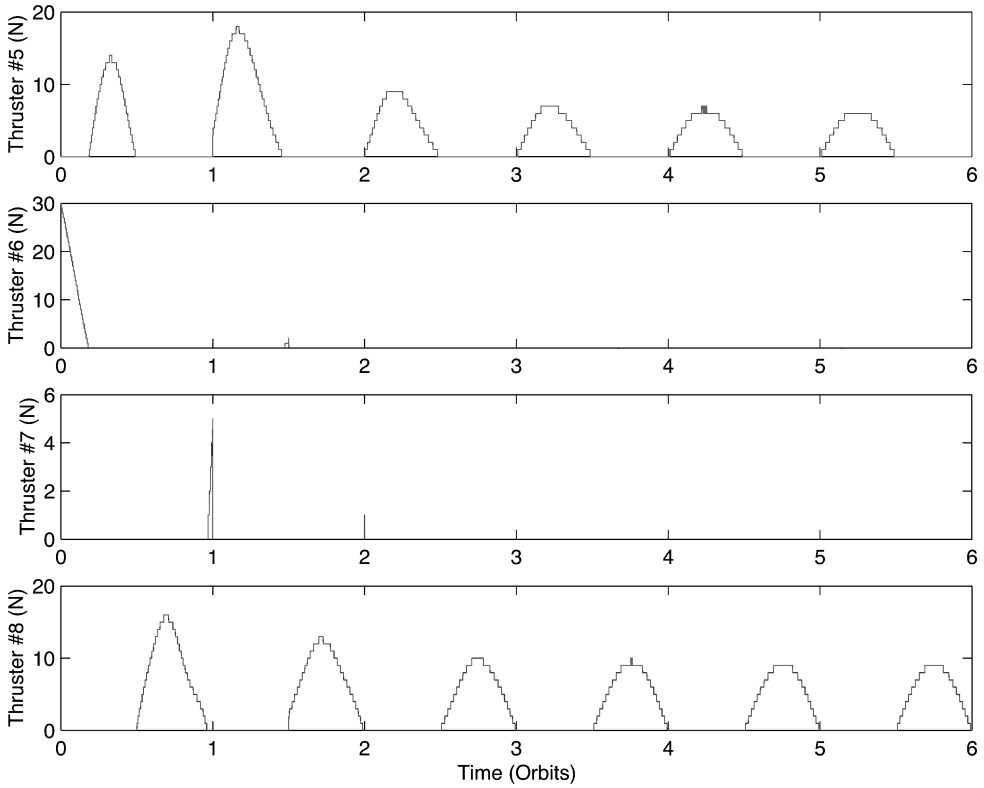

Fig. 9 Rigid-body-control simulation results for the proposed attitude-control-system architecture (continued).

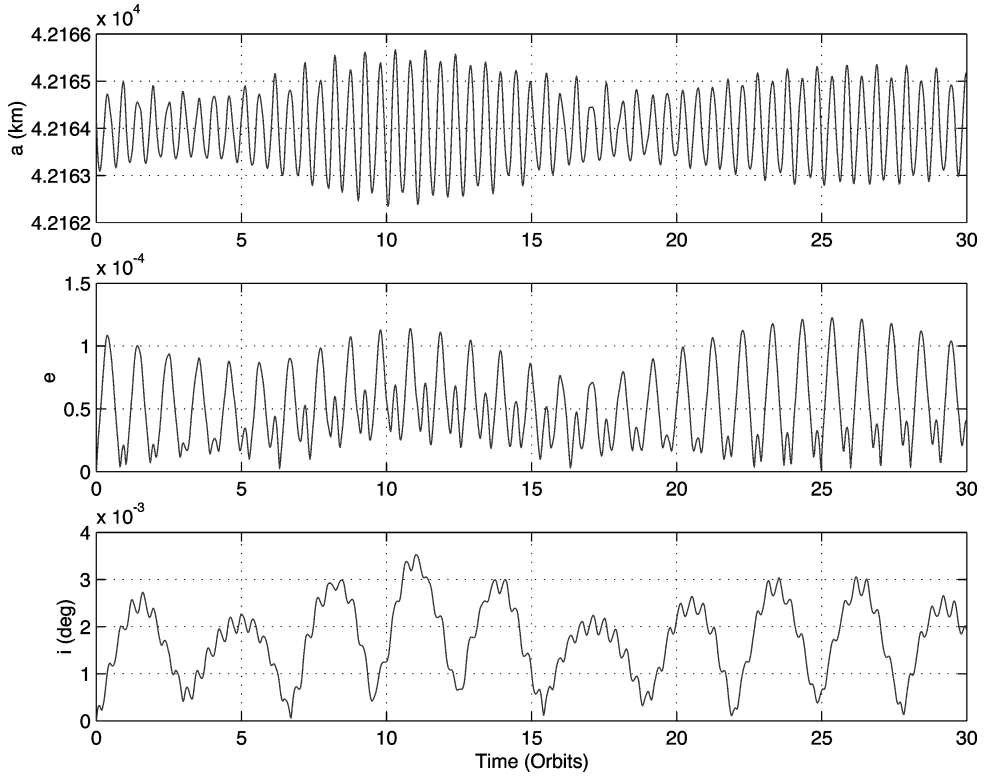

Fig. 10 Orbit simulation results with continuous (nonimpulsive) eccentricity and inclination control.

external disturbances. In this example, the closed-loop system is shown to be insensitive to dynamic modeling uncertainties of ±20%.

Although the precision microwave-beam pointing control by means of precision attitude control seems to be feasible, as demonstrated in Fig. 7, there remain the challenging engineering problems of designing a very large microwave-beam-transmitting antenna and reflector system and characterizing its precision pointing performance. The rotating reflector concept of the Abacus satellite eliminates massive rotary joint and slip rings of the 1979 SSPS reference concept; however, the lack of fine-pointing rotational joints attaching the reflector to the platform would result in very tight pointing requirements imposed on the platform itself. Consequently, further study needs to be performed for achieving the 0.1-deg microwave-beam pointing accuracy in the presence of dynamic coupling between the transmitter and reflector, Abacus platform thermal

distortion and vibrations, hardware constraints, and other short-term impulsive disturbances.

The total thrusting force from roll/pitch thrusters 1–4 nearly counters both the 60-N solar-radiation-pressure force and the cyclic pitch gravity-gradient torque; however, any residual ΔV caused by various dynamic modeling and control uncertainties should be corrected during standard north–south and east–west stationkeeping maneuvers.

As indicated in Eq. (35), the control torque needed to offset gravity-gradient torque in the pitch axis varies as $\sin 2nt$, and Fig. 8 shows that this is accomplished through alternate use of thrusters 2 and 4 to produce a force proportional to $|\sin 2nt|$. The total impulse over one orbit needed to counter the force of solar radiation pressure is $2\pi F_p/n$, which can be produced with a force whose magnitude is given by $(\pi F_p/2)|\sin 2nt|$ and whose direction is opposite to $\hat{\boldsymbol{s}}$. In addition, north–south stationkeeping can be accomplished with thrusters 5–8 delivering a force of 0.1 N opposite to the spacecraft's out-of-plane displacement. All together, the thrusters contribute to $\boldsymbol{f}$ [see Eq. (2)] a force per unit mass

$$\boldsymbol{f}_p' = -(\pi F_p/2m_B)|\sin 2nt|\,\hat{\boldsymbol{s}} - (0.1/m_B)(\boldsymbol{r}\cdot\hat{\boldsymbol{e}}_z)\hat{\boldsymbol{e}}_z$$

$$= -(\pi k/2)|\sin 2nt|\,\hat{\boldsymbol{s}} - (0.1\boldsymbol{r}\cdot\hat{\boldsymbol{e}}_z/m_B)\hat{\boldsymbol{e}}_z \tag{38}$$

The simulation described in Sec. III.D is performed again with this additional contribution, yielding the results displayed in Fig. 10, where it is evident that the secular growth in eccentricity and inclination have been eliminated. Compared to what is shown in Fig. 3, the remaining cyclic growth in eccentricity and inclination is smaller by factors of 20 and 25, respectively, thus returning the issue of stationkeeping to the realm of current solutions for geosynchronous spacecraft. As pointed out in Sec. VI.A, 85,000 kg of propellant per year is required for orbit maintenance.

The feasibility of using continuous (nonimpulsive) firings of ion thrusters for simultaneous attitude and orbit eccentricity control is demonstrated in this study; however, a further detailed orbit-control study is needed. The precision-orbit-control problem of geosynchronous satellites is a topic of continuing practical interest, as discussed in Refs. 32–35.

VII. Summary

A. Summary of Study Results

This study shows that, in addition to the well-known significant cyclic pitch gravity-gradient torque, a very large inertially oriented satellite in geostationary orbit is subject to a significant disturbance torque caused by solar radiation pressure, and the associated force produces considerable perturbation to the orbit. The Abacus satellite has an area-to-mass ratio $A/m = 0.4$ m^2/kg that is very large compared to 0.02 m^2/kg, the value associated with contemporary, higher-density spacecraft. If left uncontrolled, 60 N of solar-radiation-pressure force can cause an eccentricity increase of 0.003 and a longitude drift of 0.3 deg per month.

Attitude equations of motion of an inertially oriented spacecraft, with constant moments of inertia but with time-varying external disturbances, are developed and used for attitude control design and simulation.

The first step in meeting the objectives of the NASA SERT program regarding structural control is to avoid exciting the structure in the first place. Even though the Abacus satellite is very large and its structural frequencies are low, a requirement for precision attitude control can be met with a control bandwidth that is much lower (<orbit frequency) than the lowest structural frequency of 0.002 Hz. Hence, the significant control–structure interaction problem, which may be a major concern for such a very large, flexible Abacus platform, appears to be a tractable one. The proposed low-bandwidth attitude control system effectively utilizes a concept of cyclic-disturbance accommodating control, successfully employed for attitude control and momentum management of the ISS, to provide precision pointing of the Abacus platform in the presence of dynamic modeling uncertainties and large, but slowly varying external disturbances.

Approximately 85,000 kg of propellant per year is required for simultaneous orbit and attitude control using a minimum of 500 1-N electric propulsion thrusters with $I_{sp} = 5000$ s. The total dry mass (power processing units, thrusters, tanks, feed systems, etc.) of an electric propulsion system proposed for the Abacus satellite is estimated as 75,000 kg.

The proposed control system architecture utilizes electric thrusters, properly distributed and oriented, to counteract the large solar-radiation-pressure force. Instead of using momentum exchange devices for attitude control, the same thrusters are used to counter the secular roll torque caused by an offset of the center of mass and center of pressure; furthermore, the thrusters are employed in a cyclic fashion to oppose the cyclic pitch gravity-gradient and roll/yaw microwave-radiation torques. The resultant force and torque applied by the electric thrusters simultaneously counters the solar-radiation-pressure force and the cyclic external-disturbance torques. This represents a fundamental and novel contribution of the research reported in this paper: the propellant needed solely for orbit control is applied in such a way that attitude control is accomplished essentially at no cost.

B. Recommendations for Future Research

The baseline control system architecture developed for the Abacus satellite presupposes the availability of ion thrusters meeting certain specifications. Consequently, a 30-kW, 1-N level electric propulsion thruster with a specific impulse greater than 5000 s needs to be developed in order to avoid requiring an excessively large number of thrusters.

Several high-powered electric propulsion systems are currently under development. For example, the NASA T-220 10-kW Hall thruster recently completed a 1000-h life test. This high-power (over 5-kW) Hall thruster provides 500 mN of thrust at a specific impulse of 2450 s and 59% total efficiency. Dual-mode Hall thrusters, which can operate in either high-thrust mode or high-I_{sp} mode for efficient propellant usage, are also being developed.

The exhaust gas from an electric propulsion system consists of large numbers of positive and negative ions that form an essentially neutral plasma beam extending for large distances in space. Because little is known yet about the long-term effect of an extensive plasma on geosynchronous satellites with regard to communications, solar cell degradation, environmental contamination, etc., the use of lightweight, space-assembled large-diameter momentum wheels may also be considered as an option for the Abacus satellite; therefore, these devices warrant further study. In Table 6, the technology advances required for the Abacus satellite are summarized. It is emphasized that both electric-propulsion and momentum-wheel technologies require significant advancement to support the development of large SSPS.

Although the control–structure interaction problem appears to be tractable, further detailed study needs to be performed to achieve precision microwave-beam pointing in the presence of structural dynamical coupling between the transmitter and reflector, Abacus platform thermal distortion and vibrations, hardware constraints, and other short-term impulsive disturbances.

The lack of fine-pointing rotational joints for attaching the reflector to the antenna would result in very tight pointing requirements imposed on a very large platform. Further system-level tradeoffs will be required for design of the microwave-transmitting antenna and reflector, such as whether or not to gimbal the antenna with

Table 6 Technology advances required for the Abacus SSPS

Technology	Criteria
Electric thrusters	30 kW, 1 N $I_{sp} > 5000$ s (500–1000 thrusters)
CMGs	2000 N · m · s/kg 500,000 N · m · s/unit
Space-assembled momentum wheels	66,000 N · m · s/kg 4×10^8 N · m · s/unit (5–10 MWs)

respect to the platform, use mechanical or electronic beam steering, or employ precision-pointing rotational joints to attach the reflector to the antenna.

Acknowledgments

This paper is based on the results of a study reported in Ref. 22 and performed under NASA Contract NAS1-00122, which was monitored by Jessica Woods-Vedeler and Chris Moore at NASA Langley Research Center. The authors thank the SSP (Space Solar Power) Exploratory Research and Technology program of NASA for supporting this project. In particular, the authors are indebted to Connie Carrington, Harvey Feingold, Chris Moore, and John Mankins without whose previous SSP systems engineering work this dynamics and control research would not have been possible. Special thanks also go to Jessica Woods-Vedeler and Tim Collins at NASA Langley Research Center for their technical support and guidance throughout the course of this study.

References

[1]Glaser, P. E., "Power from the Sun: Its Future," *Science*, Vol. 162, No. 3856, 1968, pp. 857–861.

[2]Glaser, P. E., "The Potential of Satellite Solar Power," *Proceedings of the IEEE*, Vol. 65, No. 8, 1977, pp. 1162–1176.

[3]Mankins, J. C., "A Fresh Look at Space Solar Power: New Architecture, Concepts, and Technologies," 48th International Astronautical Congress, IAF-97-R.2.03, Oct. 1997.

[4]Carrington, C., Fikes, J., Gerry, M., Perkinson, D., Feingold, H., and Olds, J., "The Abacus/Reflector and Integrated Symmetrical Concentrator: Concepts for Space Solar Power Collection and Transmission," AIAA Paper 2000-3067, July 2000.

[5]Carrington, C., and Feingold, H., "Space Solar Power Concepts: Demonstrations to Pilot Plants," 53rd International Astronautical Congress of the International Astronautical Federation, IAC Paper 02-R.P.12, AIAA, Reston, VA, Oct. 2002.

[6]Battin, R. H., *An Introduction to the Mathematics and Methods of Astrodynamics*, AIAA, New York, 1987, pp. 389, 447–450.

[7]Roithmayr, C. M., "Contributions of Spherical Harmonics to Magnetic and Gravitational Fields," NASA TM-2004-213007, March 2004.

[8]Marsh, J. G., Lerch, F. J., Putney, B. H., Christodoulidis, D. C., Smith, D. E., Felsentreger, T. L., Sanchez, B. V., Klosko, S. M., Pavlis, E. C., Martin, T. V., Robbins, J. W., Williamson, R. G., Colombo, O. L., Rowlands, D. D., Eddy, W. F., Chandler, N. L., Rachlin, K. E., Patel, G. B., Bhati, S., and Chinn, D. S., "A New Gravitational Model for the Earth from Satellite Tracking Data: GEM-T1," *Journal of Geophysical Research*, Vol. 93, No. B6, 1988, pp. 6169–6215.

[9]Wie, B., *Space Vehicle Dynamics and Control*, AIAA Education Series, AIAA, Reston, VA, 1998, pp. 125, 233–239, 282–285, 290–292, 366, 367.

[10]McInnes, C. R., *Solar Sailing: Technology, Dynamics and Mission Applications*, Springer Praxis, Chichester, England, U.K., 1999, Chap. 2.

[11]Hughes, P. C., *Spacecraft Attitude Dynamics*, Wiley, New York, 1986, p. 262.

[12]Agrawal, B. N., *Design of Geosynchronous Spacecraft*, Prentice–Hall, Englewood Cliffs, NJ, 1986, pp. 70–88.

[13]Chobotov, V. A. (ed.), *Orbital Mechanics*, 3rd ed., AIAA Education Series, AIAA, Reston, VA, 2002, pp. 223–226.

[14]Chao, C. C., and Baker, J. M., "On the Propagation and Control of Geosynchronous Orbits," *Journal of the Astronautical Sciences*, Vol. 31, No. 1, 1983, pp. 99–115.

[15]Noton, M., *Spacecraft Navigation and Guidance*, Springer-Verlag, London, 1998, pp. 74, 170, 171.

[16]Bate, R. R., Mueller, D. D., and White, J. E., *Fundamentals of Astrodynamics*, Dover, New York, 1971, pp. 390–396.

[17]*The Astronomical Almanac for the Year 1999*, Nautical Almanac Office, U.S. Naval Observatory, U.S. Government Printing Office, Washington, DC, 1998, pp. D46, E4–E5.

[18]Roithmayr, C. M., "Gravitational Moment Exerted on a Small Body by an Oblate Body," *Journal of Guidance, Control, and Dynamics*, Vol. 12, No. 3, 1989, pp. 441–444.

[19]Oglevie, R. E., "Attitude Control of Large Solar Power Satellites," *Proceedings of AIAA Guidance and Control Conference*, AIAA, New York, 1978, pp. 571–578.

[20]Elrod, B. D., "A Quasi-Inertial Attitude Mode for Orbiting Spacecraft," *Journal of Spacecraft and Rockets*, Vol. 9, No. 12, 1972, pp. 889–895.

[21]Juang, J.-N., and Wang, S.-J., "An Investigation of Quasi-Inertial Attitude Control for a Solar Power Satellite," *Space Solar Power Review*, Vol. 3, No. 4, 1982, pp. 337–352.

[22]Wie, B., and Roithmayr, C. M., "Integrated Orbit, Attitude, and Structural Control Systems Design for Space Solar Power Satellites (SSPS)," NASA TM-2001-210854, June 2001.

[23]Reddy, A. S., Bainum, P. M., Krishna., R., and Hamer, H. A., "Control of a Large Flexible Platform in Orbit," *Journal of Guidance and Control*, Vol. 4, No. 6, 1981, pp. 642–649.

[24]Krishna, R., and Bainum, P. M., "Dynamics and Control of Orbiting Flexible Structures Exposed to Solar Radiation," *Journal of Guidance, Control, and Dynamics*, Vol. 8, No. 5, 1985, pp. 591–596.

[25]Rajasingh, C. K., and Shrivastava, S. K., "Orbit and Attitude Control of Geostationary Inertially Oriented Large Flexible Plate-Like Spacecraft," 37th International Astronautical Congress, IAF Paper 86-245, Oct. 1986.

[26]Wie, B., Liu, Q., and Bauer, F., "Classical and Robust H_∞ Control Redesign for the Hubble Space Telescope," *Journal of Guidance, Control, and Dynamics*, Vol. 16, No. 6, 1993, pp. 1069–1077.

[27]Wie, B., Byun, K.W., Warren, W., Geller, D., Long, D., and Sunkel, J., "New Approach to Momentum/Attitude Control for the Space Station," *Journal of Guidance, Control, and Dynamics*, Vol. 12, No. 5, 1989, pp. 714–722.

[28]Wie, B., Liu, Q., and Sunkel, J., "Robust Stabilization of the Space Station in the Presence of Inertia Matrix Uncertainty," *Journal of Guidance, Control, and Dynamics*, Vol. 18, No. 3, 1995, pp. 611–617.

[29]Wie, B., "Active Vibration Control Synthesis for the COFS (Control of Flexible Structures) Mast Flight System," *Journal of Guidance, Control, and Dynamics*, Vol. 11, No. 3, 1988, pp. 271–276.

[30]Wie, B., Horta, L., and Sulla, J., "Active Vibration Control Synthesis and Experiment for the Mini-Mast," *Journal of Guidance, Control, and Dynamics*, Vol. 14, No. 4, 1991, pp. 778–784.

[31]Wie, B., "Experimental Demonstration of a Classical Approach to Flexible Structure Control," *Journal of Guidance, Control, and Dynamics*, Vol. 15, No. 6, 1992, pp. 1327–1333.

[32]Gartrell, C. F., "Simultaneous Eccentricity and Drift Rate Control," *Journal of Guidance and Control*, Vol. 4, No. 3, 1981, pp. 310–315.

[33]Kamel, A. A., and Wagner, C. A., "On the Orbital Eccentricity Control of Synchronous Satellites," *Journal of the Astronautical Sciences*, Vol. 30, No. 1, 1982, pp. 61–73.

[34]Kelly, T. J., White, L. K., and Gamble, D. W., "Stationkeeping of Geostationary Satellites with Simultaneous Eccentricity and Longitudinal Control," *Journal of Guidance, Control, and Dynamics*, Vol. 17, No. 4, 1994, pp. 769–777.

[35]Emma, B. P., and Pernicka, H. J., "Algorithm for Autonomous Longitude and Eccentricity Control for Geostationary Spacecraft," *Journal of Guidance, Control, and Dynamics*, Vol. 26, No. 3, 2003, pp. 483–490.